This is a preprint of the book Chapter: Sabater, C. and Görtz, S. "Gradient-Based Aerodynamic Robust Optimization using the Adjoint Method and Gaussian Processes". In: Gaspar-Cunha A. et. al. Advances in Evolutionary and Deterministic Methods for Design, Optimization and Control in Engineering and Sciences. Springer. https://doi.org/10.1007/978-3-030-57422-2_14

Gradient-Based Aerodynamic Robust Optimization using the Adjoint Method and Gaussian Processes

Christian Sabater and Stefan Görtz

Abstract The use of robust design in aerodynamic shape optimization is increasing in popularity in order to come up with configurations less sensitive to operational conditions. However, the addition of uncertainties increases the computational cost as both design and stochastic spaces must be explored. The objective of this work is the development of an efficient framework for gradient-based robust design by using an adjoint formulation and a non-intrusive surrogate-based uncertainty quantification method. At each optimization iteration, the statistic of both the quantity of interest and its gradients are efficiently obtained through Gaussian Processes models. The framework is applied to the aerodynamic shape optimization of a 2D airfoil. With the presented approach it is possible to reduce both the mean and standard deviation of the drag compared to the deterministic optimum configuration. The robust solution is obtained at a reduced run time that is independent of the number of design parameters.

1 Introduction

The use of Robust Optimization in aerodynamic shape optimization is increasing in popularity in order to come up with designs less sensitive against operational and geometrical uncertainties [1, 2, 3, 4] . In opposition to deterministic optimization, where the Quantity of Interest, QoI, is a single value to be optimized, in robust optimization the QoI is a random variable. An statistic of this random variable such as the mean, combination of mean and standard deviation or quantile is usually the objective function.

When dealing with robust optimization involving expensive black box simulations, two problems are commonly present. On the one hand, the complexity of the optimization increases exponentially with the number of design parameters [5]. On the other hand, at each iteration of the optimization, a complete propagation of the uncertainty is required in order to come up with an accurate estimation of the

Christian Sabater
German Aerospace Center, DLR, Institute of Aerodynamics and Flow Technology, Lilienthalplatz 7, 38108, Braunschweig, Germany. e-mail: christian.sabatercampomanes@dlr.de

Stefan Görtz
German Aerospace Center, DLR, Institute of Aerodynamics and Flow Technology, Lilienthalplatz 7, 38108, Braunschweig, Germany. e-mail: stefan.goertz@dlr.de

statistic to be minimized [3]. A possible solution to the first problem is the use of adjoint methods [6]. Then, the gradients of the cost function with respect to all the design parameters can be efficiently obtained at a computational cost equivalent to the primal solution. To deal with the problem of uncertainty quantification, the use of surrogate methods such as Gaussian Processes can prove to be efficient to represent the stochastic space [7].

The objective of this paper is the development of a gradient-based robust design framework using the adjoint method and surrogate models and its application to the aerodynamic shape optimization of 2D airfoils.

2 Problem Definition

The problem at hand is the minimization of the drag coefficient C_D (the QoI) of the RAE 2822 airfoil against operational uncertainties.

2.1 Deterministic Optimization

For reference, a traditional deterministic optimization is computed. In this case, the aim is to find the optimum parameters $\bar{X}$ leading to the airfoil shape that minimizes the drag coefficient at a given operational conditions A.

$$\bar{X}^* = \arg\min \left\{ C_D(\bar{X}, A) \right\} \tag{1}$$

In this case, the optimization is done at constant lift coefficient, $C_L = 0.79$ and constant Mach number, $M = 0.734$. The lift coefficient constraint is enforced explicitly by iteratively varying the angle of attack during the drag evaluation in the RANS solver.

2.2 Robust Optimization

When uncertainties are present, the drag coefficient becomes a random variable. In this case, we choose to minimize a linear combination of mean, μ_{C_D} and standard deviation σ_{CD} of the drag coefficient.

$$\bar{X}^* = \arg\min \left\{ w_\mu \, \mu_{C_D}(\hat{X}, \hat{\xi}) + w_\sigma \, \sigma_{C_D}(\hat{X}, \hat{\xi}) \right\} \tag{2}$$

The value of the weights, w_μ and w_σ, are changed in order to come up with different configurations with more focus either on the mean, on its variability or on both. From a different combination of weights, a Pareto front can be obtained with the possible solutions of interest.

2.3 Parametrization

The airfoil parametrization follows Hicks-Henne deformation functions [8] that modify the camber of the airfoil. By modifying the airfoil camber, the thickness distribution is kept constant to deal with structural considerations. The vertical displacement, z_i of the camber affected by the design variable X^i can be defined as:

$$z_i = X^i \sin(\pi x^m)^3 \quad \text{where} \quad m = \frac{\log(0.45)}{\frac{i+1}{N_X+4}} \tag{3}$$

A total of $N_X = 15$ design parameters are selected. The influence of each bump function in the camber is shown in Figure 1.

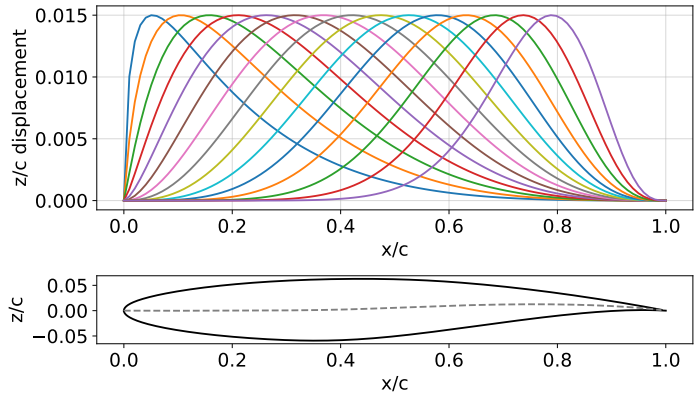

Fig. 1 Top: Fifteen Hicks-Henne Bump Function used for the parametrization. Bottom: RAE2822 shape and camber line

2.4 Uncertainties

In the robust formulation, the Mach and lift coefficient are uncertain as they are expected to slightly change during day to day aircraft operations. They are modeled as symmetric beta distributions. The mean value is centered on the nominal conditions, $\mu_M = 0.734$, $\mu_{C_L} = 0.789$, while the standard deviation is set to $\sigma_M = 0.0045$, $\sigma_{C_L} = 0.0045$. The shape parameters are the same, $\alpha_1 = \alpha_2 = 5$, in order to be symmetric, resembling truncated normal distributions. The truncation allows for a better construction of the surrogate for uncertainty quantification, and for a better representation of the physical problem. The location β_1 and scale β_2 parameters are set to have the required mean μ and standard deviation σ.

$$\text{Beta}(x) = \frac{\gamma\left(\alpha_1+\alpha_2\right)\left(\frac{x-\beta_1}{\beta_2}\right)^{(\alpha_1-1)}\left(1-\frac{x-\beta_1}{\beta_2}\right)^{(\alpha_2-1)}}{\gamma(\alpha_1)\gamma(\alpha_2)} \tag{4}$$

3 Methodology

3.1 Numerical Solver

To obtain the aerodynamic performance of the airfoil the high-fidelity DLR flow solver TAU [9] is executed on an HPC cluster system using DLR's FlowSimulator Data Manager (FSDM) environment. The Reynolds Average Navier Stokes (RANS) equations are solved using the Spalart-Allmaras turbulence model. The solution is converged when the density residual is lower than 1e-8. As shown in Figure 2, the unstructured mesh of the baseline configuration, the RAE2822 airfoil, has 29,000 grid nodes, and is quasi two-dimensional. This test case has been successfully used in the past in similar aerodynamic shape optimization problems [3, 10]. A mesh deformation tool developed by DLR using linear elasticity theory [11] is used to change the geometry at any given design vector.

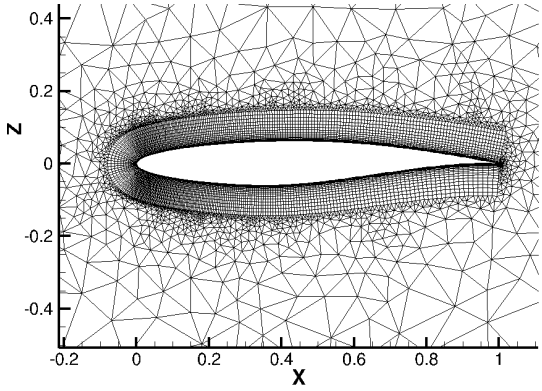

Fig. 2 Zoom-in of CFD Mesh of the RAE 2822

3.2 Adjoint Method

The adjoint formulation [6] allows to efficiently solve the total derivative of the QoI with respect to the design parameters X. This is especially useful for high

dimensional problems and few cost functions, in which the gradients can be then used for gradient-based optimization [12].

Given the minimization problem of the QoI (in this case the drag coefficient) dependent on X, the design parameters, W the flow variables and Z the mesh variables, under the constraint that the flow residual R is converged,

$$\min \{\text{QoI}(X, W, Z)\} \quad \text{s.t.} \quad R(X, W, Z) = 0 \tag{5}$$

the adjoint equation can be obtained by applying the chain rule to the lagrangian equation:

$$\frac{d\text{QoI}}{dX} = \frac{\partial \text{QoI}}{\partial Z}\frac{\partial Z}{\partial X} + \Lambda^T \frac{\partial R}{\partial Z}\frac{\partial Z}{\partial X} \tag{6}$$

where the first term is the variation of the QoI w.r.t. the shape parameter keeping the flow variables, constant. The second term is the variation of the RANS residual w.r.t. the shape parameter by keeping the flow variables constant. The adjoint variables Λ can be obtained from

$$\left(\frac{\partial R}{\partial W}\right)^T \Lambda = -\frac{\partial \text{QoI}}{\partial W} \tag{7}$$

In TAU, the discrete adjoint equations are solved [13]. After obtaining Λ, it is possible to evaluate the gradient of the QoI w.r.t. the design parameters. When dealing with optimization at constant lift the gradients w.r.t. the QoI, the drag coefficient C_D must be corrected [14] :

$$\left.\frac{dC_D}{dX}\right|_{C_L=C_{L_0}} = \frac{\partial C_D}{\partial X} - \frac{\partial C_D}{\partial \alpha}\frac{\partial \alpha}{\partial C_L}\frac{\partial C_L}{\partial X} \tag{8}$$

The adjoint method has been validated wrt. finite differences for the baseline configuration. Figure 3 shows the gradient of the drag coefficient at constant lift with respect to each of the 15 design parameters for both the adjoint and forward finite differences. Despite the small differences, mainly due to the use of forward instead of central finite differences, the adjoint formulation is able to accurately obtain the desired gradients, reducing the run time by 83%.

3.3 Surrogate Based Uncertainty Quantification

The main problem of uncertainty quantification is the large number of function evaluations required to propagate the uncertainty of the input parameters (in this case operational conditions) to the QoI (drag coefficient) at any given design, $\bar{X}_j$ [1]. To directly perform Monte Carlo Simulations is prohibitive when using CFD solvers. A typical approach is then the use of surrogates of the stochastic space for example, through Polynomial Chaos Expansion or Gaussian Processes.

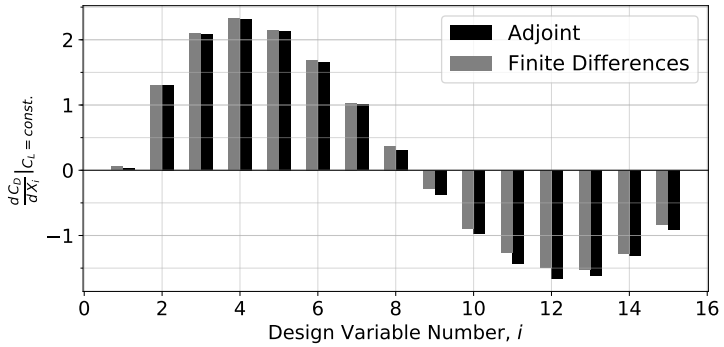

Fig. 3 Comparison of the gradients of the drag obtained with finite differences and the adjoint

Gaussian Processes models, GPs (also known as Kriging) have been traditionally used in aerodynamic shape optimization as surrogate models for global optimization [15]. However, these have been recently used as non-intrusive approach to perform uncertainty quantification due to its good capability to globally represent the stochastic space [10, 16].

The main idea of UQ in Gaussian Processes is as follows: at a given configuration, $\bar{X}_j$, an initial design of experiments (DoE) sampling in the stochastic space $\bar{\xi}$ (in this case random operating conditions), is evaluated in the full order model. Based on this sampling, the GP is built. Then, a large number (N_K) of Quasi Monte Carlo samples can be cheaply evaluated in the surrogate to obtain the statistic, such as the mean or standard deviation of the drag, following equation 9,

$$\mu_{\text{QoI}}(\bar{X}_j) = \frac{1}{N_K}\sum_{k=1}^{N_K} \hat{\text{QoI}}(\bar{X}_j, \bar{\xi}_k) \qquad \sigma_{\text{QoI}}(\bar{X}_j) = \sqrt{\frac{1}{N_K}\sum_{k=1}^{N_K}\left[\hat{\text{QoI}}(\bar{X}_j, \bar{\xi}_k) - \mu_{\text{QoI}}\right]^2} \tag{9}$$

where $\hat{\text{QoI}}\left(\bar{X}_j, \bar{\xi}_k\right)$ is obtained by prediction of the surrogate built in the stochastic space $\bar{\xi}$.

3.3.1 Statistics of the Gradients

If the deterministic gradients of the QoI with respect to the design parameters at a given point $\bar{X}_j$ are also available, $\frac{d\text{QoI}}{dX^i}\Big|_{\bar{X}_j, \bar{\xi}_k}$, the gradients of the statistics can also be obtained. In this case a surrogate model needs to be built per each design parameter X^i. For example, the gradient of the mean value of the QoI with respect to a given design parameter X^i at any given design point $\bar{X}_j$, $\frac{d\mu_{\text{QoI}}}{dX^i}\Big|_{\bar{X}_j}$, can be obtained from:

$$\left.\frac{d\mu_{\mathrm{QoI}}}{dX^i}\right|_{\bar{X}_j} = \frac{1}{N_K}\sum_{k=1}^{N_K}\left.\frac{d\hat{\mathrm{QoI}}}{dX^i}\right|_{\bar{X}_j,\bar{\xi}_k} \tag{10}$$

In this case the deterministic gradients $\left.\frac{d\hat{\mathrm{QoI}}}{dX^i}\right|_{\bar{X}_j,\bar{\xi}_k}$ are obtained from direct integration on the given surrogate according to the design parameter X^i.

The gradient of the standard deviation of the QoI respect to each design parameter has also an analytical expression:

$$\left.\frac{d\sigma_{\mathrm{QoI}}}{dX^i}\right|_{\bar{X}_j} = \frac{1}{N_K\,\sigma_{\mathrm{QoI}}(\bar{X}_j)}\sum_{k=1}^{N_K}\left(\hat{\mathrm{QoI}}(\bar{X}_j,\bar{\xi}_k)-\mu_{\mathrm{QoI}}(\bar{X}_j)\right)\left(\left.\frac{d\hat{\mathrm{QoI}}}{dX^i}\right|_{\bar{X}_j,\bar{\xi}_k}-\left.\frac{d\mu_{\mathrm{QoI}}}{dX^i}\right|_{\bar{X}_j,\bar{\xi}_k}\right)^2 \tag{11}$$

Then, the stochastic space can be characterized for both the QoI (C_D), that is obtained by the primal solution of the CFD solver, and for each of the different N_x gradients of the QoI with respect to the design parameters, that are efficiently obtained by the adjoint method. As shown in Figure 4, $N_X + 1$ different surrogates are constructed, one to obtain the statistics of the primal solution and N_X to obtain the statistics of each of the gradients.

3.3.2 Proposed Approach

To construct the surrogate, samples follow a DoE strategy following Sobol Sequences [17]. Sobol Sequences are a low discrepancy, quasi-random sequence that use a base of two to successively create uniform partitions of the unit interval [17]. The sampling is normalized to the distribution of the input uncertainties, ξ. As a result, more samples will be placed along the mean than in the tails of the input distributions. Locations that will be recalled more often when integrating the surrogate with Monte Carlo will be more accurate than those that have less probability of being evaluated.

The Gaussian Process model consists of Universal Kriging with a Gaussian Kernel (exponent fixed to 2). They hyperparameters of the correlation model are tuned according to the maximization of the model likelihood through Differential Evolution. The Surrogate-Modelling for Aero-Data Toolbox (SMARTy) developed by DLR is used for the initial Design of Experiments sampling and for the creation of the Kriging surrogate [18].

To increase the accuracy of the statistics, after the DoE, an active infill criteria that deals with sampling evenly in the stochastic space [19] is used. Gaussian Processes provide the estimation of the surrogate error at any given point in the stochastic space, $\hat{s}(\bar{\xi})$ [15]. Then, new samples are added in the location $\bar{\xi}_k^*$ where the product of the probability distribution function of the input parameters, PDF_X times the error estimation of the error is maximized. The optimum location is found in the surrogate through Differential Evolution.

$$\bar{\xi}_k^* = \arg\min_{\bar{\xi}} \left\{ -\text{PDF}_X(\bar{\xi}) \ \hat{s}(\bar{\xi}) \right\} \tag{12}$$

Additional samples are added until convergence on the statistics of the QoI. This is achieved by assessing the error of the statistic that is integrated in the surrogate, $\hat{s}_\mu$ through the Monte Carlo evaluation in both the upper bound, $\hat{\text{QoI}}(\bar{\xi}) + \hat{s}(\bar{\xi})$, and lower bound, $\hat{\text{QoI}}(\bar{\xi}) - \hat{s}(\bar{\xi})$, prediction given by the surrogate. From here, the upper μ_{QoI}^U and lower μ_{QoI}^L estimation of the statistic are respectively obtained. The difference between upper and lower bound (variability in the determination of the statistics) is associated to the statistical error.

$$\hat{s}_\mu = \frac{\mu_{\text{QoI}}^U - \mu_{\text{QoI}}^L}{2} \tag{13}$$

3.4 Optimization Framework

As shown in Figure 4, the optimization framework combines the gradients obtained by the adjoint formulation with the uncertainty quantification using GPs.

A Sequential Least Squares Programming (SQP) gradient based optimizer is used. At any given design point, $\bar{X}_j$, the optimizer requires both the statistic and its gradients w.r.t. the design parameters $\bar{X}$. Then, at each iteration, the uncertainty quantification is performed in the stochastic space with the help of the surrogate in order to obtain the statistic of the QoI (drag coefficient in this case). A Gaussian Process is also built for each individual dimension in order to obtain the gradient of the statistic of the QoI w.r.t. to the design parameters following equations 10 and 11. For example, if the focus is in the mean value, both μ_{QoI} and $\frac{d\mu_{\text{QoI}}}{d\bar{X}}$ are efficiently obtained at each iteration.

This approach differs from the one in which a global surrogate such as Gradient Enhanced Kriging [18] is built, whose values and derivates are computed by the primal and the adjoint. In that case, the global surrogate accuracy and construction time would be very sensitive to the number of dimensions, N_X. When dealing with more complex problem with hundreds of dimensions, only the training time of the global surrogate would make the approach unfeasible. The strength of the proposed method is that decouples the dimensionality in the design space from the surrogate accuracy, as this one is built only in the stochastic space with a reduced number of samples. As each surrogate of the gradients is built independently for each dimension, the training time only increases linearly with the number of design parameters.

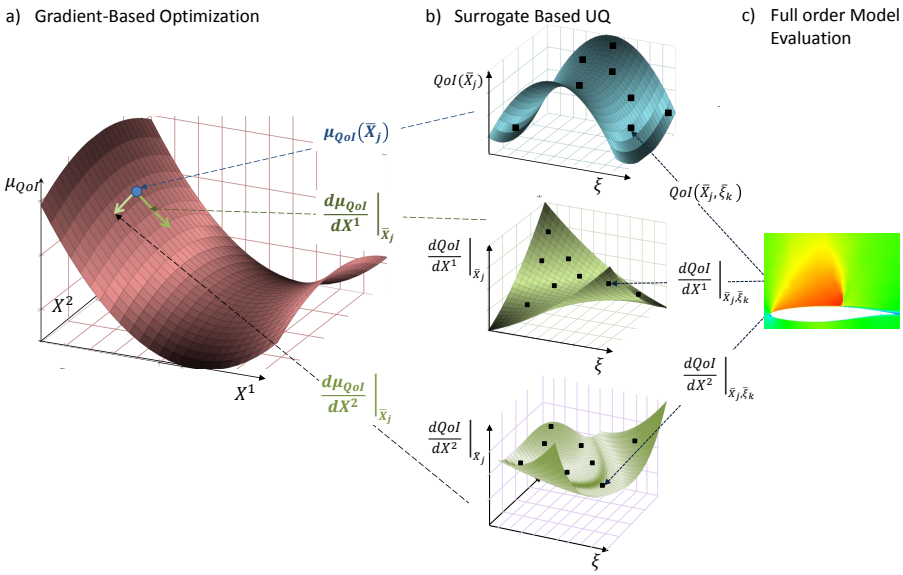

Fig. 4 Robust Design Framework using the Adjoint and Gaussian Process: a) Gradient Based Optimization of the mean of the QoI; b) Uncertainty Quantification through Gaussian Processes of the C_D and each of its gradients; c) Evaluation of each deterministic solution in full order model

4 Results

4.1 Deterministic Optimization

Figure 5 shows the convergence history of the gradient-based deterministic optimization using the adjoint. The optimization starts with the initial RAE2822 configuration. A total of 19 Iterations are required. The optimum configuration decreases the drag coefficient by 34.9%, from to 191.3 drag counts to 124.58 drag counts. According to the pressure coefficient distribution of Figure 6, the reduction in drag follows mainly to the weakening of the strong normal shock wave of the original configuration.

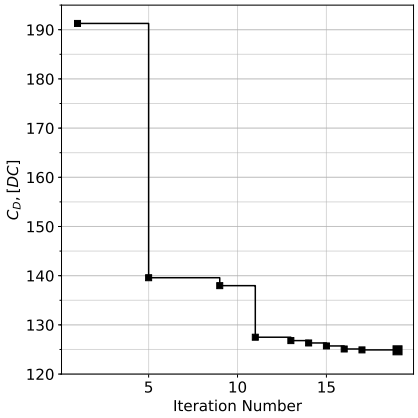

Fig. 5 Convergence History of deterministic Gradient Based Optimization.

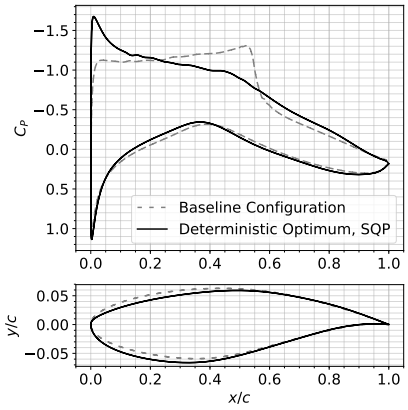

Fig. 6 Pressure coefficient for baseline and optimum configurations.

4.2 Uncertainty Quantification

To study the accuracy of the proposed uncertainty quantification on GPs, the deterministic optimum configuration is perturbed under uncertainty. To obtain the reference statistics (mean and standard deviation) of this configuration, 10,000 Quasi Monte Carlo Samples are evaluated in the CFD model. Based on that, it is possible to obtain the accuracy of the statistics provided by the surrogate for a given number of training samples required to construct them.

Figure 7 a show the convergence in the absolute error between the reference mean and the one obtained with the surrogate built from a given number of samples, for different infill strategies. In general, as the surrogate is built with more and more samples, the mean value is obtained more accurately. However, when only a DoE approach is followed, the accuracy of the surrogate is reduced. For a given computational budget, the use of the infill is preferred. In addition, it is better to start the infill after a good global exploration by using 10 DoE samples. Finally, an error smaller than 0.2 drag counts is desired in order to have a stable convergence during the optimization and provide useful results. According to this, a minimum of 12 to 15 samples are required when the active infill is valid, while if using only a DoE strategy, the required number of samples increases to 24.

The same conclusions can be obtained for the convergence error of the standard deviation in Figure 7 b. When dealing with higher order moments such as the standard deviation the accuracy requirements are more challenging. In this case, the use of the infill criteria is necessary to come up with a good accuracy of the standard deviation.

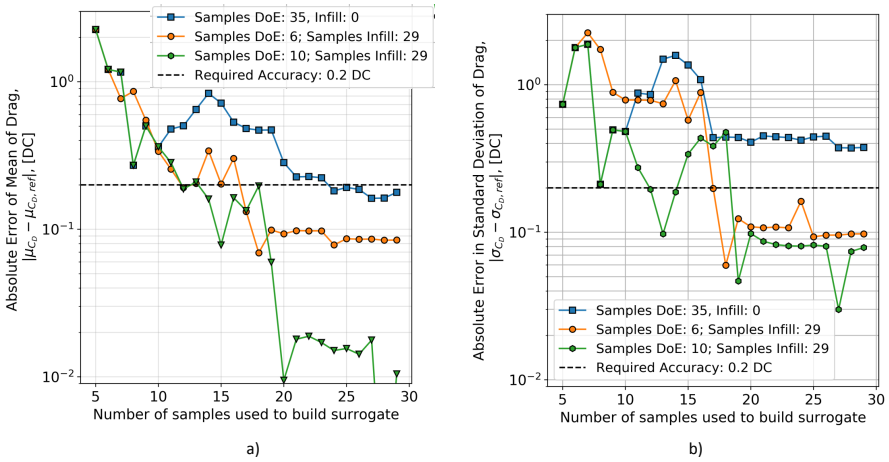

Fig. 7 Convergence history of the statistical error according to the number of samples used to build the surrogate on: a) mean; b) standard deviation

4.3 Robust Optimization

The robust optimization is repeated six times with different weights for the mean and standard deviation following the framework introduced in Section 3. Each optimum configuration is obtained at a reduced computational cost, requiring from 17 to 24 iterations of the gradient-based optimizer. At each iteration, 14 to 16 CFD samples are required to accurately obtain the statistics of the drag through the surrogate approach. Then, a total of 200 to 400 CFD evaluations are required to obtain a optimum robust configuration.

The Pareto-Optimal solutions in terms of mean and standard deviation of drag is shown in Figure 8. The deterministic optimum configuration behaves poorly under uncertainty, and has both higher mean and standard deviation than two of the robust configurations. From an engineering point of view, the configuration with similar weights in mean and standard deviation, ($w_\mu = 1, w_\sigma = 1.5$) looks appealing. By slightly increasing the mean value of the drag, its variability can be reduced by half. There is a clear trade-off between configurations less sensitive to drag, and configurations with a good average performance. Keeping in mind that the gradient based method only guarantees local optimality, the framework is able to provide a set of non-dominated robust solutions in which a designer can choose from. This can only be achieved when the accuracy of the statistics (specially the standard deviation) and its gradients is high.

The probability distributions and box plots of the stochastic drag is shown in the violin plot Figure 9 for the different configurations. On top of each distribution, the mean value is also highlighted in white. The deterministic solution (grey) has a mean value of 129.6 drag counts and a standard deviation of 4.7 drag counts, while the robust solution with focus on the mean value displaces further down the histogram

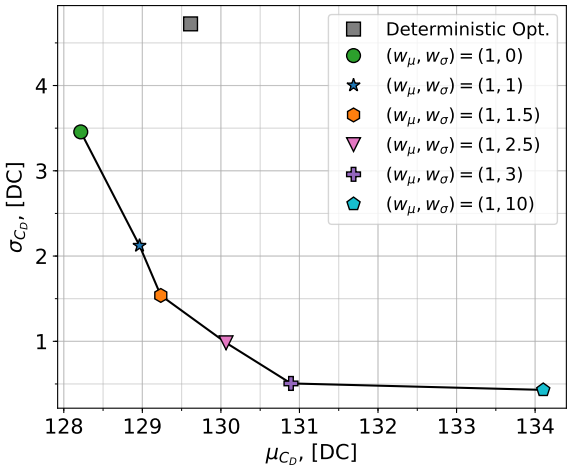

Fig. 8 Pareto Front of standard deviation and mean of drag coefficient for optimum configurations

towards a mean value of 128.2 and standard deviation of 3.5 drag counts. However, in both cases a large tail is present towards higher values of drag. When more importance is placed in the standard deviation, solutions have a peaky distribution and the tail is decreased, at an expense of a larger mean value, as previously shown in the Pareto front.

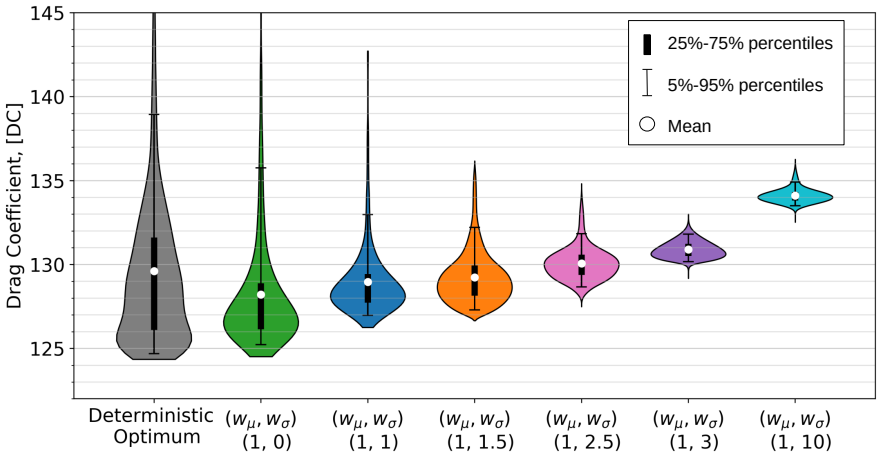

Fig. 9 Violin plot of drag coefficient for the configurations of interest

The different airfoil shapes are shown in Figure 10. All the optimum configurations have an increased curvature near their leading edge compared to the baseline airfoil. This allows for a better expansion of the flow and elimination of the strong shock

wave over the upper surface. Despite small, there are some differences between the deterministic and robust airfoils.

The robust airfoils have an increased curvature of around 60% to 70% of the chord. This is similar to adding a "shock control bump" device, that is able to smear stronger shock waves when the Mach and Lift randomly increase w.r.t. nominal conditions. The curvature or "bump" is larger in the designs when variability must be minimized.

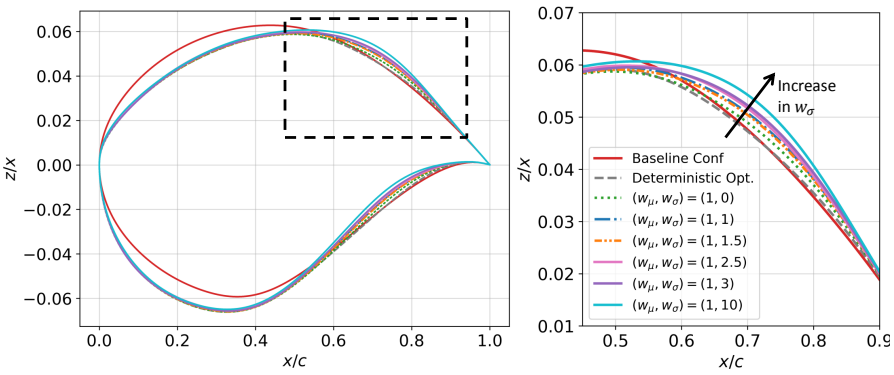

Fig. 10 Airfoil shapes of the configurations of interest

The standard deviation of the pressure field is shown in Figure 11 for the robust optimum with focus on the mean ($w_\mu = 1, w_\sigma = 0$, configuration A) and for the one with strong focus on the variation, ($w_\mu = 1, w_\sigma = 10$, configuration B). For each configuration, the field has been obtained by superimposing 300 snapshots of the flow solution computed with Monte Carlo.

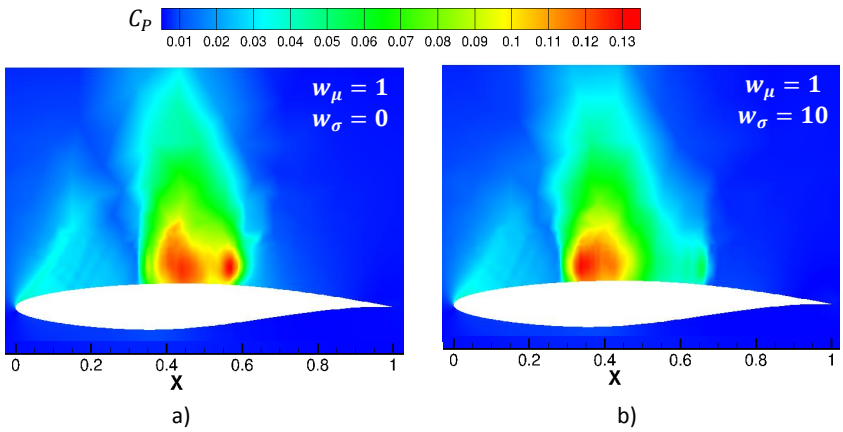

Fig. 11 Standard deviation of the pressure coefficient field for Robust configurations: a) Focus on mean; b) Focus on standard deviation

There is a larger longitudinal variation of the shock wave along the airfoil in configuration A, as the focus was on the mean drag and not on the standard deviation. In addition, this variation is stronger. In this case, two shock wave patterns can be present around 40% to 60% of the chord. Configuration B on the other hand reduces the displacement of the shock wave and moves it further upstream, around 35% to 45% of the chord, due to the stronger curvature previously discussed. However, as the shock wave is further upstream, the average drag increases.

5 Conclusions

A novel gradient-based robust optimization method has been presented and applied to a test case. The combination of a CFD adjoint code with Gaussian Process can be used to efficiently obtain the gradients of the mean and standard deviation of the drag coefficient with respect to the design parameters. This reduces both the number of optimization iterations, and the samples required for uncertainty quantification.

The application to aerodynamic shape optimization shows that the deterministic optimum, under uncertainty, behaves poorly. In order to come up with more realistic configurations, a robust formulation is required. A multi-objective approach in which the mean and standard deviation of the drag compete against each other is an attractive approach for the design of robust configurations. There is a trade-off among the configurations less sensitive to the drag, and those with a lower average drag.

This method should be preferred in optimizations when the number of design parameters is much larger compared to the number of uncertainties. Compared to deterministic gradient-based optimization, the addition of uncertainty increases the computational time by a factor of 10 to 15. However, as the framework is independent to the number of design parameters, it is readily available for the robust optimization of more complex 3 dimensional configurations.

Under more uncertainties, the use of Gradient Enhanced Kriging, which takes the gradients of the uncertain parameters to build the surrogate in the stochastic space, will increase the accuracy of UQ. In the future, other robustness measures such as the quantile will be investigated. The framework will also be applied to the optimization of 3D wings under a large number of design parameters, where it will show its full potential.

Acknowledgments

This work is funded by the European Commission's H2020 programme, through the UTOPIAE Marie Curie Innovative Training Network, H2020-MSCA-ITN-2016, Grant Agreement number 722734.

References

1. Duvigneau, R. Aerodynamic shape optimization with uncertain operating conditions using metamodels. resreport RR-6143, INRIA (2007).
2. Schulz, V. & Schillings, C. Optimal aerodynamic design under uncertainty. In *Notes on Numerical Fluid Mechanics and Multidisciplinary Design*, 297–338 (Springer Berlin Heidelberg, 2013).
3. Maruyama, D., Liu, D. & Goertz, S. An efficient aerodynamic shape optimization framework for robust design of airfoils using surrogate models. In *Proceedings of the VII European Congress on Computational Methods in Applied Sciences and Engineering (ECCOMAS Congress 2016)* (NTUA Greece, 2016).
4. Kumar, D., Raisee, M. & Lacor, C. Combination of polynomial chaos with adjoint formulations for optimization under uncertainties. In *Uncertainty Management for Robust Industrial Design in Aeronautics*, 567–582 (Springer International Publishing, 2018).
5. Shan, S. & Wang, G. G. Survey of modeling and optimization strategies to solve high-dimensional design problems with computationally-expensive black-box functions. *Structural and Multidisciplinary Optimization* **41**, 219–241 (2009).
6. Giles, M. B. & Pierce, N. A. An introduction to the adjoint approach to design. *Flow, turbulence and combustion* **65**, 393–415 (2000).
7. Maruyama, D., Goertz, S. & Liu, D. General introduction to surrogate model-based approaches to UQ. In *Uncertainty Management for Robust Industrial Design in Aeronautics*, 203–211 (Springer International Publishing, 2018).
8. Hicks, R. M. & Henne, P. A. Wing design by numerical optimization. *Journal of Aircraft* **15**, 407–412 (1978).
9. Gerhold, T. Overview of the hybrid RANS code TAU. In *MEGAFLOW - Numerical Flow Simulation for Aircraft Design*, 81–92 (Springer Berlin Heidelberg, 2015).
10. Sabater, C. & Goertz, S. An efficient bi-level surrogate approach for optimizing shock control bumps under uncertainty. In *AIAA Scitech 2019 Forum* (American Institute of Aeronautics and Astronautics, 2019).
11. Gerhold, T. & Neumann, J. The parallel mesh deformation of the DLR TAU-code. In *Notes on Numerical Fluid Mechanics and Multidisciplinary Design (NNFM)*, 162–169 (Springer Berlin Heidelberg, 2006).
12. Brezillon, J. & Dwight, R. P. Applications of a discrete viscous adjoint method for aerodynamic shape optimisation of 3d configurations. *CEAS Aeronautical Journal* **3**, 25–34 (2011).
13. Dwight, R. Efficiency improvements of rans-based analysis and optimization using implicit and adjoint methods on unstructured grids. *DLR Deutsches Zentrum fur Luft- und Raumfahrt e.V. - Forschungsberichte* (2006).
14. Reuther, J., Jameson, A., Farmer, J., Martinelli, L. & Saunders, D. Aerodynamic shape optimization of complex aircraft configurations via an adjoint formulation. In *34th Aerospace Sciences Meeting and Exhibit* (American Institute of Aeronautics and Astronautics, 1996).
15. Forrester, A. I. & Keane, A. J. Recent advances in surrogate-based optimization. *Progress in Aerospace Sciences* **45**, 50–79 (2009).
16. Maruyama, D., Liu, D. & Goertz, S. Surrogate model-based approaches to UQ and their range of applicability. In *Uncertainty Management for Robust Industrial Design in Aeronautics*, 703–714 (Springer International Publishing, 2018).
17. Sobol, I. On the distribution of points in a cube and the approximate evaluation of integrals. *USSR Computational Mathematics and Mathematical Physics* **7**, 86–112 (1967).
18. Han, Z.-H., Goertz, S. & Zimmermann, R. Improving variable-fidelity surrogate modeling via gradient-enhanced kriging and a generalized hybrid bridge function. *Aerospace Science and Technology* **25**, 177–189 (2013).
19. Dwight, R. & Han, Z.-H. Efficient uncertainty quantification using gradient-enhanced kriging. In *50th AIAA/ASME/ASCE/AHS/ASC Structures, Structural Dynamics, and Materials Conference* (American Institute of Aeronautics and Astronautics, 2009).